

Long-Term Video Generation of Multiple Futures Using Human Poses

Naoya Fushishita
fushishita@mi.t.u-tokyo.ac.jp
The University of Tokyo

Antonio Tejero-de-Pablos
antonio-t@mi.t.u-tokyo.ac.jp
The University of Tokyo

Yusuke Mukuta
mukuta@mi.t.u-tokyo.ac.jp
The University of Tokyo, RIKEN

Tatsuya Harada
harada@mi.t.u-tokyo.ac.jp
The University of Tokyo, RIKEN

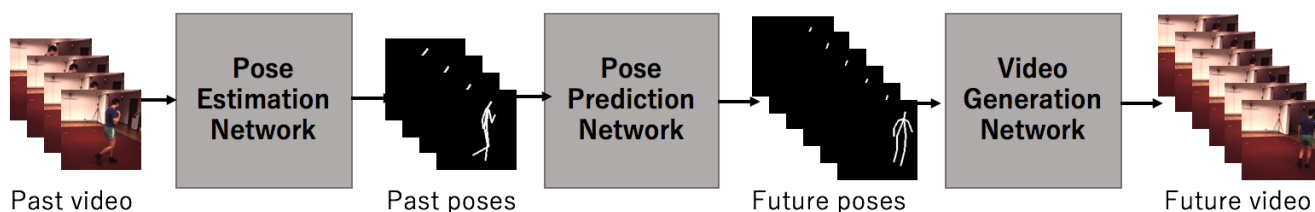


Figure 1: Overview of the proposed method. First, human pose in the input video is estimated. From this, multiple plausible human poses are predicted for a long-term near-future. Finally, the future video based on the predicted poses is generated.

ABSTRACT

Predicting the near-future from an input video is a useful task for applications such as autonomous driving and robotics. While most previous works predict a single future, multiple futures with different behaviors can possibly occur. Moreover, if the predicted future is too short, it may not be fully usable by a human or other system. In this paper, we propose a novel method for future video prediction capable of generating multiple long-term futures. This makes the predictions more suitable for real applications. First, from an input human video, we generate sequences of future human poses as the image coordinates of their body-joints by adversarial learning. We generate multiple futures by inputting to the generator combinations of a latent code (to reflect various behaviors) and an attraction point (to reflect various trajectories). In addition, we generate long-term future human poses using a novel approach based on unidimensional convolutional neural networks. Last, we generate an output video based on the generated poses for visualization. We evaluate the generated future poses and videos using three criteria (i.e., realism, diversity and accuracy), and show that our proposed method outperforms other state-of-the-art works.

CCS CONCEPTS

• **Information systems** → **Multimedia content creation**; • **Computing methodologies** → **Image representations**; **Reconstruction**; **Machine learning**.

KEYWORDS

future video prediction, long-term video generation, human pose, generative adversarial networks

1 INTRODUCTION

Predicting the immediate-future from observed visual information has wide applications (e.g., robotics, autonomous cars). In particular, when developing a machine that interacts with humans, incorporating future prediction is useful to prevent accidents. Therefore, predicting human behavior is a remarkably important, but also challenging task, since several requirements have to be met. First, since sometimes future is uncertain, there are multiple plausible futures that may occur. Thus, future prediction methods that predict only one future [4, 27] out of a range of plausible events, are not suitable to certain real world situations (e.g., an autonomous car that sees a pedestrian on the road). Also, if the predicted future implies a dangerous situation, it is necessary to handle it appropriately. If we want to avoid a dangerous future, short-term predictions may not provide a time span long enough to handle the situation, and thus, relatively long predictions are desirable (e.g., an autonomous car predicts an accident but cannot stop in time). Furthermore, in case that predictions are interpreted by humans, predictions need to be in an interpretable form, such as natural language sentences or videos. Especially, videos contain a lot of information, and thus, many prior works try to generate videos predicting the future [17, 18].

This paper presents a novel method for video prediction of multiple futures from a given input human video. The predicted future is long-term (about two to four times longer than short-term future prediction [18, 29]). We also tackle the generation of the video representing the predicted future. Before generating the future videos, our method first predicts future poses from the human present in the input video. There are two reasons for this approach. First, when generating long video from scratch (i.e., without pose information)

using 3D convolutional neural networks, objects with complex motion such as humans tend to disappear or collapse [28]. Second, considering applications involving interaction with humans, such as robotics and autonomous cars, prediction of human behavior has higher priority than other objects.

Many existing works tackle the task of predicting future human pose from an input human pose by using Recurrent Neural Networks (RNNs) [10, 12, 27, 29]. However, when predicting long-term poses, training an RNN takes a considerably long time because RNNs training cannot be parallelized. RNNs also suffer from the problem of vanishing gradients, which hampers learning of long data sequences. So, for long-term pose generation, we use unidimensional convolutional neural networks (1D CNN) instead of RNNs. We generate predictions of plausible future poses via generative adversarial learning [11]. However, adversarial learning suffers from mode collapse, in which only a few or a single data are generated. We introduce a latent code [7] representing different behaviors to be able to generate multiple poses. Also, we include a location condition on the generated poses, so human motion is attracted towards different points of the image.

Our contributions are as follows.

- We propose a novel method for future human video prediction. We predict multiple futures by (1) imposing a condition to generate various types of motions, and (2) imposing a condition to generate motions towards various locations in the image.
- In order to handle long-term future prediction of human behavior, we propose a novel approach for generating human pose sequences using unidimensional convolutional networks.
- We provide extensive evaluation of the proposed method to validate our results, and a comparison with state-of-the-art works.

2 RELATED WORK

In recent years, future video prediction has been approached by methods based on Generative Adversarial Networks (GANs) [11].

2.1 Generative adversarial networks

GAN is a generative model in which a discriminator tries to classify between fake data produced by a generator or real data. The learning finishes when the generator fools completely the discriminator. While the output of GAN is generated from latent noise and cannot be controlled, Conditional GAN (CGAN) [19] includes an input label that conditions the generated data. InfoGAN[7] unsupervisedly models the relationships between the latent code and the generated images by maximizing the mutual information between them. This allows to apply variations to the generated images without requiring an input label. However, these networks suffer from mode collapse, that is, the model ends up generating only a single or a few predominant data.

2.2 Automatic video generation

GANs have been mainly used for image and video generation tasks, being the latter more challenging since consecutive frames have to be coherent. Vondrick et al. [28] proposed Video GAN, which

generates a foreground video, a background image, and a mask video to merge them. In order to improve coherence in motion and appearance, Ohnishi et al. [21] proposed Flow and Texture GAN, which generates optical flow first and then the appearance of the video in a hierarchical architecture. Instead of generating a video from random latent variables, Mathieu et al. [18] approached the task of generating a video as a continuation of the a video input as a condition. Later, Lee et al. [17] generated multiple future videos from the same input video.

2.3 Human pose prediction

Human motion prediction aims to generate plausible future human behavior from a human behavior input such as coordinates or angles of human joints. Although many prior works that approached this task [1, 2, 25, 30], recent developments in deep learning provided an improvement in the results. Fragkiadaki et al. [10] proposed the Encoder-Recurrent-Decoder model to predict future human poses, which consists of a long short-term memory (LSTM, a kind of RNN) [13], an encoder and a decoder. Similarly, Bütepage et al. [4] predicted future human poses using an autoencoder-like model. Gui et al. [12] proposed a method for future human pose prediction based on adversarial networks with a gated recurrent unit (GRU, a kind of RNN) [8]. While many previous works employ RNNs, these suffer from the vanishing gradients problem: the longer the path between two elements, the worse forward and backward signal propagation [15, 26]. Also, small errors in the output of the LSTM are propagated, and accumulated when generating long sequences. This makes them unsuitable for learning long-term pose sequences.

2.4 Future video generation using human pose

One of the most successful approaches for generating human video is by using a human pose input. Yan et al. [31] generated future video from an input frame and a given sequence of future human poses. Villegas et al. [27] first predicted future human poses as body-joint coordinates using an LSTM and then generated video frame by frame based on generated pose. This approach succeeded in generating long-term videos, but cannot generate multiple futures because the output of an LSTM does not vary for the same input. Cai et al. [5] proposed an adversarial network that generates human pose sequences from latent noise and an action class label, and a network that generates video from the generated poses. This model can be extended to generate a future pose given a past pose, but cannot generate a variety of multiple futures. Also, using an action class label is unsuitable for future prediction since the behavior of the human may not follow a specific action pattern. Walker [29] combined an LSTM and a variational autoencoder (VAE) [16] to generate multiple human poses from a pose sequence input, and then generate a video using 3D convolutional neural networks. The VAE allows generating multiple human poses, which are then fed to the LSTM to predict a sequence of future poses. However, this approach is unsuitable for long-term future prediction because errors in the LSTM will be accumulated exponentially.

In this paper, we propose a method for long-term video prediction of multiple futures. In order to generate long-term near-future sequences, we leverage unidimensional convolutional neural networks, which allow generating sequences without suffering from

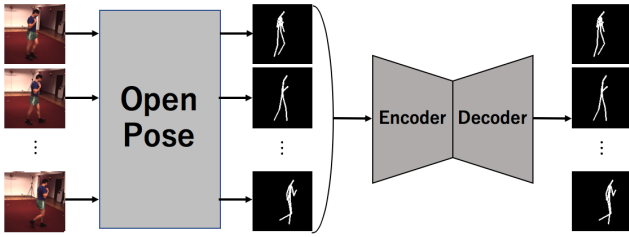


Figure 2: Overview of our pose estimation network. Human poses in the input video are estimated using OpenPose [6]. Then, an autoencoder network corrects wrongly estimated poses.

the vanishing gradients and error propagation problems. Then, we encourage our network to generate a variety of multiple futures by using two conditions; a latent code that induces a type of motion, and an attraction point that induces motion towards a location in the image.

3 METHODOLOGY

Figure 1 shows an overview of our method, which consists of three networks that are trained independently. First, our pose estimation network provides the human pose in a given input video. Then, our pose prediction network generates future human pose sequences that are smooth, varied and long. Finally, our video generation network generates future video corresponding to the generated poses. Since the duration of our predicted human poses is comparatively long, and represent a variety of multiple futures, the generated videos show the same characteristics.

3.1 Pose estimation network

We show an overview of our pose estimation network in Figure 2. Our pose estimation network estimates the position of the body joints of the human in the video in image coordinates (xy) . Several networks have been proposed in the past [6, 20]; we use OpenPose [6], which has been widely utilized in a variety of related applications. However, Openpose sometimes provides wrong estimations (e.g., missing joints). Thus, we introduce an autoencoder network to correct the estimated coordinates. This network consists of an encoder and a decoder, which consist of two fully connected layers each. The network is trained using a dataset with annotations of human joint coordinates (see Section 4.1), by minimizing the mean squared error between estimated coordinates and those of the ground truth.

3.2 Pose prediction network

Our pose prediction network takes our estimated poses as input and generates future pose sequences. Our generated pose sequences are smoothly connected to the input poses, they have a long-term duration, and represent a variety of multiple futures.

Figure 3 shows an overview of our pose prediction network. It consists of three modules: a pose generator (G_p), a global pose discriminator (D_{pg}), and a local pose discriminator (D_{pl}). Let $p_t \in \mathbf{R}^{2N}$ be the human pose at time step t . Here, N is the number of

joints that compose the pose, and p_t is a vector containing the xy coordinates of N joints at time step t . The input of G_p is a latent noise z , the input poses from a T frames-long video $P_{in} = (p_0, p_1, \dots, p_{T-1})$, a latent code c , and an attraction point $a \in \mathbf{R}^2$ (c and a are explained later). The output of G_p is a sequence of T' future human poses $\hat{P}_{gen} = (\hat{p}_T, \hat{p}_{T+1}, \dots, \hat{p}_{T+T'-1})$ that follow P_{in} .

The structure of the network is based on CGAN [19]; the input poses are included as a condition to G_p , D_{pg} and D_{pl} . However, our method contains two major modifications. First, we use two discriminators, one global and one local. Whereas D_{pg} tries to discriminate if the generated sequence of T' poses are real or fake, D_{pl} tries to discriminate a short subsequence of T'' poses ($T'' < T'$). The global discriminator pays attention to only the overall flow of the sequence, but since we generate long-term future, it may overlook spontaneous erroneous poses. Introducing a local discriminator that pays attention to short-term details allows our network to generate smoother and more realistic pose sequences. Second, we use unidimensional convolutional neural networks (1D CNNs) in our generator and discriminators. Although many previous works [10, 12, 27, 29] used RNNs (i.e., LSTM and GRU) for predicting future human pose sequences, 1D CNNs have advantages over RNNs. Whereas RNNs need to be trained sequentially (i.e., one instance at a time), CNNs can be trained in parallel, reducing the execution cost. Also, 1D CNNs can model distant time relationships without being as sensitive as RNNs to the problem of vanishing gradients (see Section 2.3). Whereas RNNs need $\mathcal{O}(t)$ steps to predict an element separated t frames from the input, 1D CNNs with a stride width of s need only $\mathcal{O}(\log_s t)$ layers. Since the problem of vanishing gradients (see Section 2.3) gets worse with the number of steps/layers, 1D CNNs seem more suitable to model long-term relationships. In image generation with a 2D CNN [22], an image is regarded as a three-dimensional entity $\in \mathbf{R}^{H \times W \times 3}$ and convoluted in height and width direction using a two dimensional filter. In our generation task with a 1D CNN, we regard a pose sequence as a two-dimensional entity $P \in \mathbf{R}^{T \times 2N}$ (each row is an individual pose p) and convolute it in the height (time) direction with a one-dimensional filter.

CGAN suffers from mode collapse, that is, the generator fails to adequately cover the space of possible predictions and instead generates one or a few prominent modes, ignoring the latent variables. Thus, only modifying the latent noise z is not enough to generate multiple varied pose sequences. To tackle this problem, our method includes two additional inputs to the generator, namely the latent code c and the attraction point a . Both are randomly initialized during training, and then used during testing for pose generation from different combinations of c and a . InfoGAN [7] models the relationship between the latent code c and the generated data $G(z, c)$ in an unsupervised way, by maximizing the mutual information between them. Since human actions can be categorized to some extent (e.g., "walking" or "sitting"), we aimed at establishing a correspondence between such action categories and the latent code, and thus, we represent c as a one-hot vector. The attraction point a represents the xy coordinates of a point in the image space, and used to train G_p to generate poses towards the attraction point. This allows our method to generate multiple varied pose sequences depending on a , which in turn is chosen randomly. When generating pixel-based

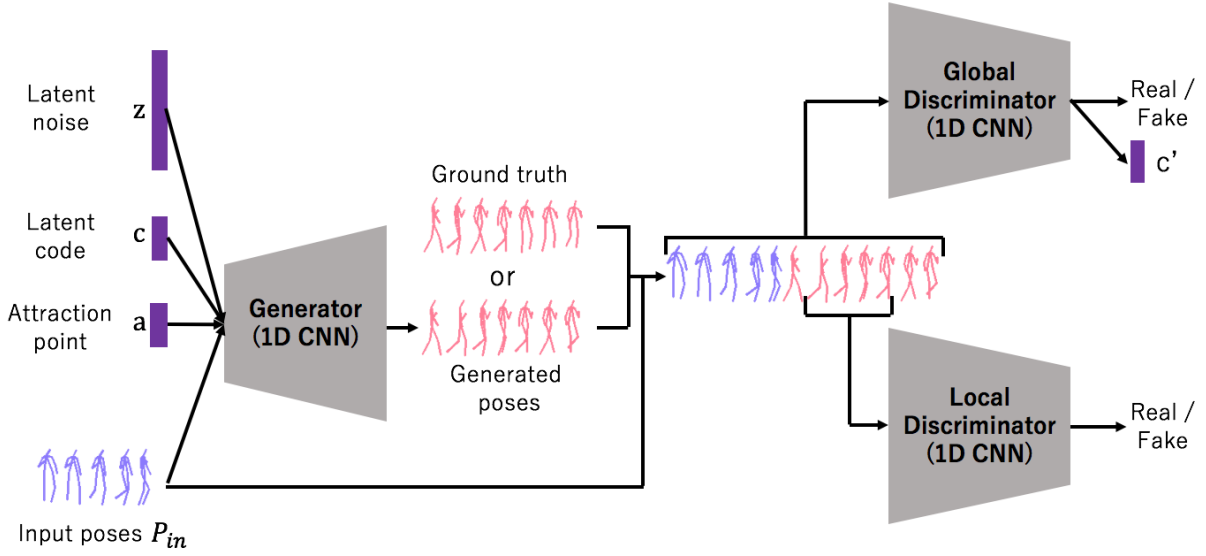


Figure 3: Overview of pose prediction network. It generates future pose sequence from past pose sequence given as condition. To generate long pose, we use two discriminators and use 1D CNN in generator and discriminators. We generate diverse pose sequences by changing latent code and attraction point randomly.

data (i.e., image or video), applying this kind of constraint explicitly is not intuitive, but for our joint-coordinates generation task is possible.

Training. During training, G_p tries to fool both discriminators by generating plausible future pose sequences, while D_{pg} and D_{pl} try to classify whether the pose sequences are real or generated. The objective function for adversarial learning between G_p , D_{pg} and D_{pl} is as follows:

$$\begin{aligned} \mathcal{L}_{adv} = & \mathbb{E}_{P_{gt}}[\log D_{pg}(P_{gt}|P_{in})] + \mathbb{E}_{P_{gt}}[\log D_{pl}(P_{gt},l)] + \\ & \mathbb{E}_{z,c,a}[\log(1 - D_{pg}(G_p(z,c,a|P_{in})|P_{in}))] + \\ & \mathbb{E}_{z,c,a}[\log(1 - D_{pl}(G_p(z,c,a|P_{in})|l))] \end{aligned} \quad (1)$$

P_{in} is the input pose sequence and P_{gt} is ground truth for the future pose sequence.

The objective function to maximize the mutual information between latent code c and generated poses is:

$$\mathcal{L}_c = - \sum_{i=1}^C c_i \ln Q(c'|G_p(z,c,a|P_{in}))_i \quad (2)$$

As in [7], D_{pg} estimates the latent code c from $G_p(z,c,a)$. $Q(c'|G_p(z,c,a))$ is the distribution learned by D_{pg} from the generated data to latent code and C is the number of categories.

Our generator G_p is trained to minimize the distance between the generated poses and the attraction point a . More concretely, it minimizes the distance between a and the generated coordinate of the waist joint at future frame t' : $\hat{p}_{T+t',waist}$.

$$\mathcal{L}_a = \frac{1}{T'} \sum_{t'=0}^{T'-1} \|a - \hat{p}_{T+t',waist}\|_2^2 \quad (3)$$

In addition, in order to generate smoother pose sequences, we introduce a loss that reduces sudden speed changes between adjacent poses.

$$\mathcal{L}_{diff} = \frac{1}{T'-2} \sum_{t'=0}^{T'-3} \|(\hat{p}_{T+t'+2} - \hat{p}_{T+t'+1}) - (\hat{p}_{T+t'+1} - \hat{p}_{T+t'})\|_2^2 \quad (4)$$

In summary, the overall objective function is:

$$\min_{G_p, Q} \max_{D_{pg}, D_{pl}} \mathcal{L} = \mathcal{L}_{adv} + \lambda_c \mathcal{L}_c + \lambda_a \mathcal{L}_a + \lambda_{diff} \mathcal{L}_{diff} \quad (5)$$

where λ s are coefficients to weight the contribution of each loss.

Implementation. In our implementation, T (the length of the input pose sequences) is 16, T' (the length of the output pose sequences) is 128 and T'' (the length of the input pose sequences to D_{pl}) is 16. C (the number of categories of the latent code c) is 15. G_p consists of seven unidimensional convolutional layers and D_{pg} and D_{pl} consist of three unidimensional convolutional layers and one linear layer. D_{pg} has additional two linear layers to estimate c' . All the unidimensional convolutional layers have a kernel size of 4, a stride of 2, and a padding of 1. We set $\lambda_c = 10$, $\lambda_a = 50$ and $\lambda_{diff} = 100$.

3.3 Video generation network

Figure 4 shows an overview of our video generation network. Our video generation network generates future frames with respect to a past frame and our predicted future pose sequence, following an adversarial approach. We use an architecture based on [31]. It generates a single future frame from two inputs, namely the last frame of the input video x_T and a generated future pose $p_{t'}$. The final video is obtained by repeating this for all T' future frames.

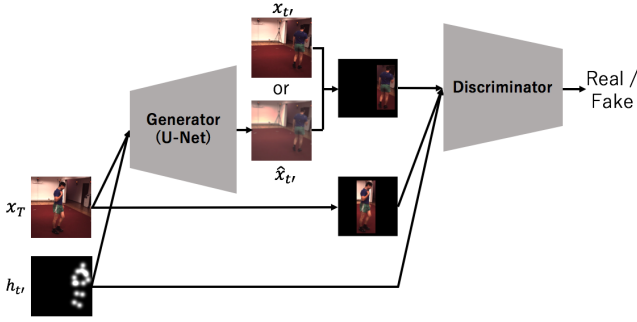


Figure 4: Overview of our video generation network. Each future frame $\hat{x}_{t'}$ is generated from the last frame of the input video x_T and the heatmap of the generated future pose $h_{t'}$. Input images to the discriminator are masked to show only the area around the predicted poses, so that the discriminator can focus on the human.

Not generating the whole video directly at once [28] but generating each frame individually increases the image quality.

Before being input to the video generation network, the human pose coordinates generated by the pose prediction network $p_{t'}$ are transformed into a heatmap $h_{t'}$. Our heatmaps have N channels, in which each channel represents the position of each joint using a Gaussian distribution centered in the predicted xy coordinates. Thus, for a future frame t' , the frame generator G_f takes the last input RGB frame x_T and the predicted future pose $h_{t'}$. Our G_f follows the U-Net architecture [23]. Inputs x_T and $h_{t'}$ are concatenated in the channel direction. G_f encodes the image with $3 + N$ channels and decodes it into the future frame $\hat{x}_{t'}$. Then, our frame discriminator D_f takes the input image x_T , the generated future pose $h_{t'}$, and either the real future frame $x_{t'}$ or the generated future frame $\hat{x}_{t'}$ and discriminates whether future frame is real or fake (i.e., generated). Since generating a realistic human is more difficult than generating the background, D_f should focus on the foreground human. Therefore, we mask D_f input images to show only the area where the human appears, delimited by the outermost joint coordinates (Fig. 4).

Training. When training our video generation network, instead of using the poses generated by the pose prediction network, we use the poses from the ground truth data. We use three kinds of objective functions, as in [31]. The first one is the adversarial loss:

$$\mathcal{L}_{adv} = \mathbb{E}_{x_{t'}, x_T, p_{t'}} [\log D_f(x_{t'}, x_T, p_{t'})] + \mathbb{E}_{x_T, p_{t'}} [\log(1 - D_f(G_f(x_T, p_{t'}), x_T, p_{t'}))] \quad (6)$$

The second one is the mean absolute error between the pixels in the ground truth video and the generated video:

$$\mathcal{L}_{L_1} = \frac{1}{M} \|x_{t'} - G_f(x_T, p_{t'})\|_1^2 \quad (7)$$

where M is the total number of pixels in each frame.

Lastly, the triplet loss [24] ensures proper continuity among video frames. Triplet loss addresses three images (i.e., an anchor, a positive and a negative) and minimizes the distance between an anchor and a positive and maximizes the distance between an

anchor and a negative. In a video, the L2 distance of adjacent frames should be smaller than that of distant frames. Therefore, when the anchor is $\hat{x}_{t'}$, we set $\hat{x}_{t'+1}$ as positive and $\hat{x}_{t'+5}$ as negative. The concrete objective function is:

$$\mathcal{L}_{tri} = \frac{1}{M} [\|\hat{x}_{t'} - \hat{x}_{t'+1}\|_2^2 - \|\hat{x}_{t'} - \hat{x}_{t'+5}\|_2^2 + \alpha]_+ \quad (8)$$

In summary, the overall objective function is:

$$\min_{G_f} \max_{D_f} \mathcal{L} = \mathcal{L}_{adv} + \lambda_{L_1} \mathcal{L}_{L_1} + \lambda_{tri} \mathcal{L}_{tri} \quad (9)$$

where λ s are coefficients to weight the contribution of each loss.

Implementation. G_f consists of an encoder and a decoder, which are connected with skip connections. The encoder and the decoder consist of eight convolutional layers. The first layer of the encoder and the last layer of decoder have a kernel size of 3, a stride of 1, and a padding of 1. The other layers have a kernel size of 4, a stride of 2, and a padding of 1. We set $\lambda_{L_1} = 10000$ and $\lambda_{tri} = 1000$.

4 EXPERIMENTS

Evaluating generated video is not straightforward, and normally a single metric is insufficient. In our method, the diversity of the generated futures is an important criterion, but it is not enough and to predict the future of ground truth is also important. In addition, video quality should also be evaluated. Following the evaluation in [17], we evaluate generated poses and videos from three criteria: realism, diversity and accuracy.

4.1 Dataset

We use the Human3.6M [14] dataset to train and evaluate our entire pipeline. Videos in this dataset show 11 actors showing different behavior (e.g., *walking*, *sitting*). All frames are annotated with the real and image coordinates of 32 body joint positions accurately measured via motion capture. We use 720 videos corresponding to subjects 1, 5, 6, 7, 8 and 9 as train data and 120 videos of subject number 11 as test data.

We preprocess the videos in the following manner. In order to enlarge actors, videos are cropped by using the outermost poses in the entire sequence, and then resized into 128×128 patches. Since Human3.6M videos have a high frame rate, motion between adjacent frames is small. Therefore, we subsample the video uniformly by taking one every four frames. We apply two kinds of data augmentation. One is horizontal video flipping. The other is padding frames with black pixels, and randomly cropping patches of size 128×128 containing the human. Since our method masks the human of the input image to the discriminator (see Section 3.3), this augmentation is not harmful for our method. We use 14 joints out of the 32 provided: *head*, *neck*, *right shoulder*, *right elbow*, *right wrist*, *left shoulder*, *left elbow*, *left wrist*, *right waist*, *right knee*, *right foot*, *left waist*, *left knee* and *left foot*. In all experiments, an input of 16 frames long is used to generate future videos of 128 frames long generated as a continuation of the input.

4.2 Comparison with the related work

To the best of our knowledge, there is no other work on long-term multiple future video generation, so we compare the performance of our method with two state-of-the-art works in long-term future

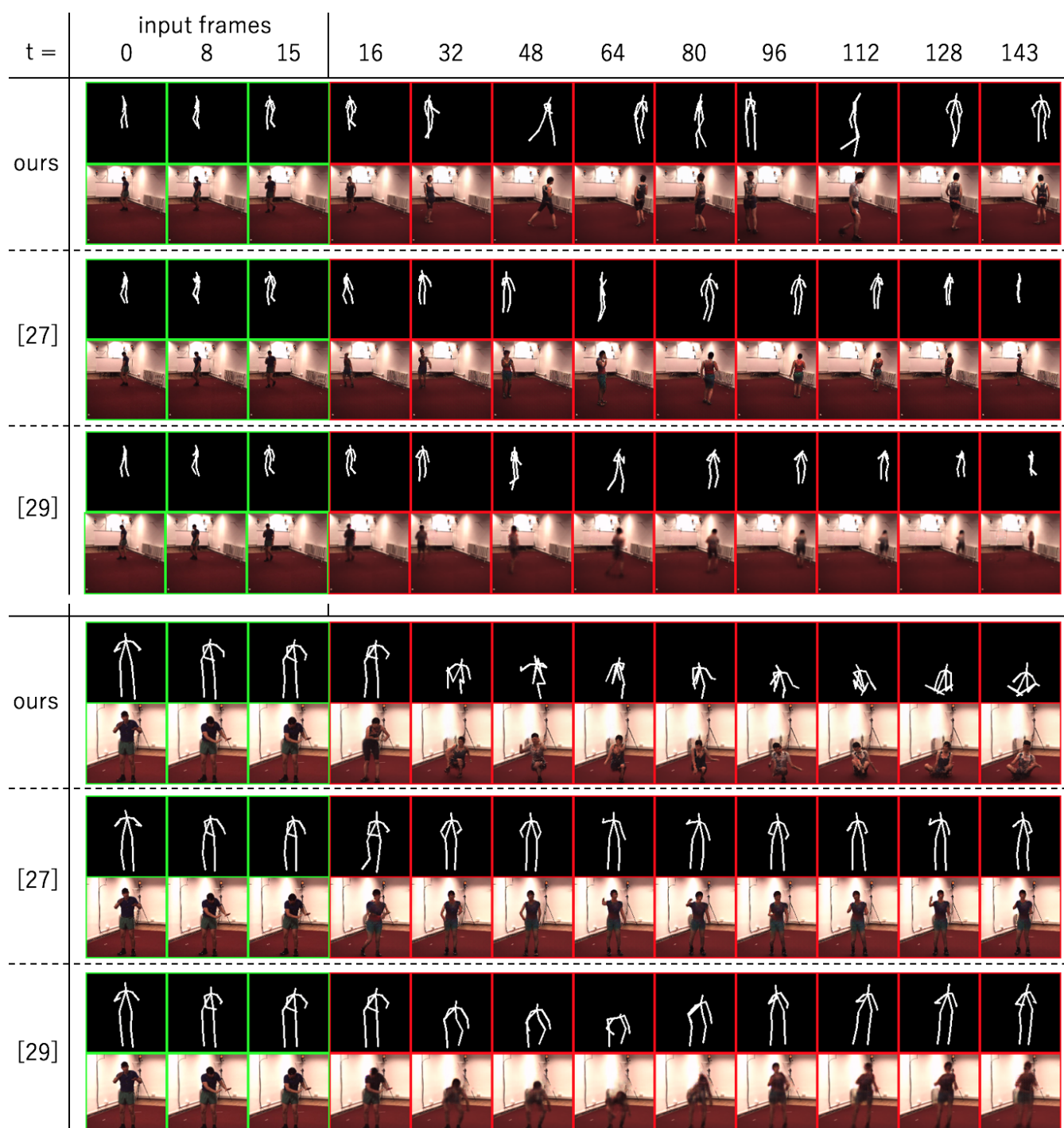


Figure 5: Examples of generated poses and frames. Input frames are marked in green and generated frames are marked in red. Pose sequences generated by [27] contain less motion (in the walking video, the generated person does not move their legs, although they move forward), and the connection between input poses and generated poses is not smooth. The first few video frames generated by [29] are realistic, but the later frames are blurred compared to ours and [27]. Our method and [27], which generate videos frame by frame, have a lower consistency in the person’s clothes color than [29], which generates an entire video. This could be avoided by employing a dataset with a greater variety of clothes.

Table 1: Percentage of workers that preferred futures generated by our method.

	vs. [27]	vs. [29]
Pose	61.0	54.3
Video	50.2	66.0

video generation and multiple future generation respectively. On the one hand, [27] predicts long-term future poses by using an LSTM and then generates the video frame by frame. This method avoids error propagation in long sequences since the predicted poses are not input back, but is not capable of generating multiple futures. On the other hand, [29] predicts multiple future poses by using an LSTM and a VAE, and then generates the entire video using a 3D CNN. This method does not seem to be suitable for generating long-term future video, since the predicted poses are repeatedly input back to the LSTM, which causes errors to accumulate.

4.3 Realism of the generated futures

In this experiment, we evaluate the realism of generated futures via a user study on Amazon Mechanical Turk (AMT). We show workers a pair of future poses or a pair of future videos generated by our proposed method and [27] or [29], and workers select the one that looks more realistic. 600 pairs of poses/videos each were evaluated by 60 workers.

Table 1 shows the experimental results. We outperformed both [27] and [29] in terms of the realism of the generated poses and videos. Table 1 suggests superiority of our pose prediction network, which leverages a unidimensional CNN to predict long-term poses. Compared to [27], our generated poses were preferred, but for videos there is almost no difference. Both [27] and our method generate long-term future frames from the past frame x_T and a future pose $p_{t'}$. The further t' gets from T , the harder generating complex poses $p_{t'}$ is. Unlike [27], we generate multiple futures that contain a variety of motions, which makes them harder to generate. Also, users preferred our videos to those of [29]. The first few frames of the videos generated by [29] have a good quality, but rest of the frames tend to be blurry.

4.4 Diversity of the generated futures

We evaluated the diversity of the predicted futures by calculating the distance between futures generated from the same input video. The more varied the futures are, the larger the distance. We calculate the distance between two future poses as the mean squared error (MSE) of the image coordinates of their 14 joints. Besides, we calculate the distance between two future videos as the cosine distance of the feature vectors from VGG16 (pretrained by ImageNet [9]). This distance is calculated as the average of the five cosine distances between the feature vectors of each of the five pooling layers of VGG16. The L2 distance between the pixels of two videos is another possible distance. However, humans tend to recognize two videos different when different objects exist or different movements are performed. Whereas feature vectors of VGG16 are more sensitive to image content, L2 distance is more sensitive to visual

Table 2: Evaluation about the diversity of generated poses and videos.

Method	Pose (MSE)	Video (Cosine)
[29]	0.0181	0.1447
ours (w/o c , w/o a)	0.0001	0.0399
ours (w/o c , w/ a)	0.0984	0.3961
ours (w/ c , w/o a)	0.0861	0.3732
ours (w/ c , w/ a)	0.1256	0.4266

attributes such as brightness. Thus, using cosine distance of feature vector of VGG16 is in line with human intuition.

Our method is able to generate multiple futures by leveraging a latent code c and an attraction point a . Therefore, we evaluate diversity in four ways: with c and a , with c and without a , without a and with c , without c and a . Also, we compare the results with the multiple futures generated with [29]. Since [27] cannot generate diverse futures, it is not included in this evaluation.

Table 2 shows the obtained results. When we disabled both the latent code c and the attraction point a , mode collapse occurs and the average distance between two samples is remarkably small. On the other hand, the greatest distance is obtained when using both c and a . From this, we can conclude that our latent code and attraction point are effective to generate multiple futures.

4.5 Accuracy of the generated futures

Since one of the goals of this research is to generate multiple futures, in principle generating futures far from the ground truth future is not a problem. However, it is desirable that some futures among the variety generated are close to the ground truth. Hence, we generate 100 future poses and videos from the same input video, and measure their distance with the ground truth. Similarity between poses is calculated using the MSE of the image coordinates of the joints (the lower the MSE the higher the similarity). Similarity between videos is calculated as the cosine distance of the feature vectors of VGG 16, and the peak signal-to-noise ratio (PSNR). We use the PSNR distance to measure frame differences at the pixel level. We compare the accuracy of the four combinations of adding the latent code c and the attraction point a , and the methods in [27] and [29].

Figure 6 shows the similarity metrics between the ground truth and the video among the generated one hundred with the highest similarity to the ground truth. With respect to the pose accuracy, using c and a allows for a wider variety of generated poses, thus, there is a higher chance that futures resembling the ground truth are generated. The results suggest that our two additional inputs are effective for not only generating multiple futures but also generating accurate futures. With respect to the video accuracy, although our method outperforms [29] in terms of both accuracy of poses and realism of videos, the video accuracy is very similar. The reason is that future videos in [29] reflect better pixel colors in the input video, despite being blurry (and thus, less realistic).

5 CONCLUSIONS AND FUTURE WORK

In this work, we present a novel method for generating long-term future videos of multiple futures from an input human video using

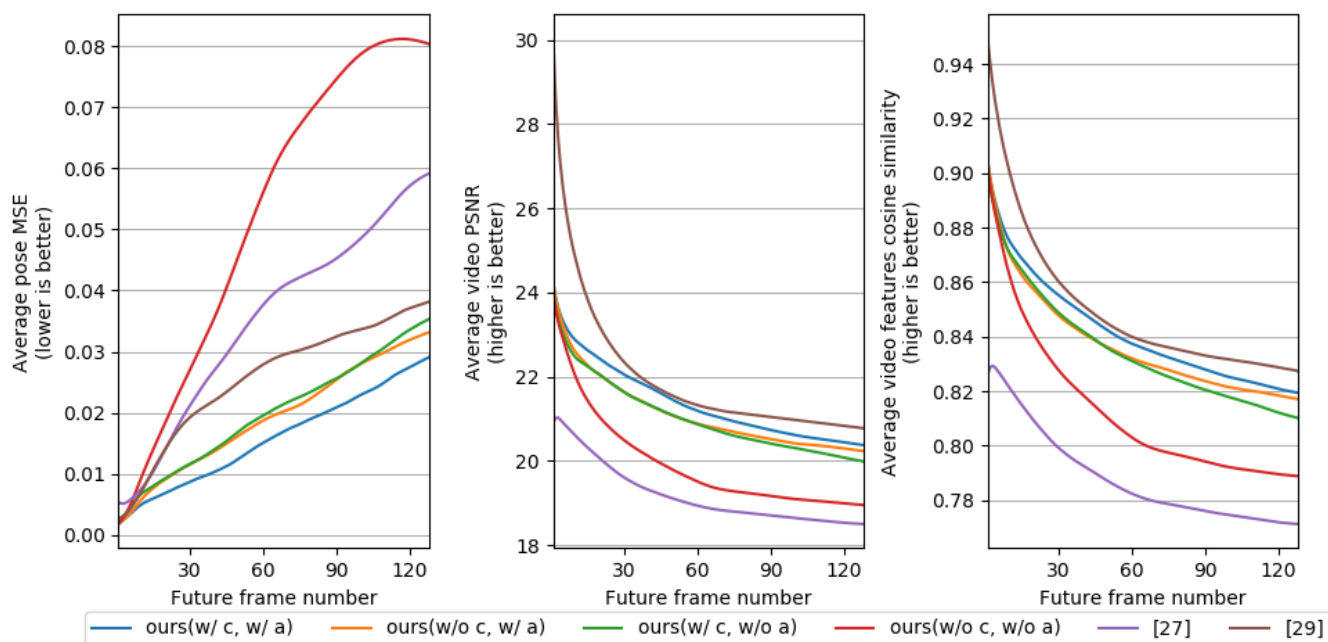


Figure 6: Comparison of the similarity between the generated futures (poses and videos) and the ground truth.

a hierarchical approach: first predicting future human poses and then generating the future video. We propose a novel network to predict long-term future human pose sequences by using unidimensional convolutional neural network in adversarial training. Also, we propose two additional inputs that allow predicting a variety of multiple futures: a latent code and an attraction point. Finally, videos generated with our predicted poses are also long and multiple. Experimental results on the realism, diversity, and accuracy of the generated poses and videos show the superiority of the proposed method over the state-of-the-art.

As our future work, since our method generates videos frame by frame, videos with a higher resolution could be generated by leveraging the latest image generation techniques using GAN [3]. Also, we plan to tackle the limitations of our method; for example, generating videos with moving background, and generating videos different from humans.

ACKNOWLEDGMENTS

This work was partially supported by JST CREST Grant Number JPMJCR1403, Japan, and partially supported by the Ministry of Education, Culture, Sports, Science and Technology (MEXT) as "Seminal Issue on Post-K Computer."

REFERENCES

- [1] Ijaz Akhter, Tomas Simon, Sohaib Khan, Iain Matthews, and Yaser Sheikh. 2012. Bilinear spatiotemporal basis models. *ACM Transactions on Graphics* 31, 2 (2012), 17.
- [2] Matthew Brand and Aaron Hertzmann. 2000. Style machines. In *ACM International Conference on Computer Graphics and Interactive Techniques*.
- [3] Andrew Brock, Jeff Donahue, and Karen Simonyan. 2019. Large scale gan training for high fidelity natural image synthesis. *arXiv preprint arXiv:1809.11096* (2019).
- [4] Judith Bütepage, Michael J Black, Danica Kragic, and Hedvig Kjellström. 2017. Deep representation learning for human motion prediction and classification. In *Computer Vision and Pattern Recognition*.
- [5] Haoya Cai, Chunyan Bai, Yu-Wing Tai, and Chi-Keung Tang. 2018. Deep Video Generation, Prediction, and Completion of Human Action Sequences. In *European Conference on Computer Vision*.
- [6] Zhe Cao, Tomas Simon, Shih-En Wei, and Yaser Sheikh. 2017. Realtime multi-person 2d pose estimation using part affinity fields. In *Computer Vision and Pattern Recognition*.
- [7] Xi Chen, Yan Duan, Rein Houthoofd, John Schulman, Ilya Sutskever, and Pieter Abbeel. 2016. InfoGAN: Interpretable Representation Learning by Information Maximizing Generative Adversarial Nets. In *Neural Information Processing Systems*.
- [8] Kyunghyun Cho, Bart van Merriënboer, Çağlar Gulcehre, Dzmitry Bahdanau, Fethi Bougares, Holger Schwenk, and Yoshua Bengio. 2014. Learning Phrase Representations using RNN Encoder-Decoder for Statistical Machine Translation. In *Empirical Methods in Natural Language Processing*.
- [9] Jia Deng, Wei Dong, Richard Socher, Li-Jia Li, Kai Li, and Li Fei-Fei. 2009. Imagenet: A large-scale hierarchical image database. In *Computer Vision and Pattern Recognition*.
- [10] Katerina Fragkiadaki, Sergey Levine, Panna Felsen, and Jitendra Malik. 2015. Recurrent network models for human dynamics. In *International Conference on Computer Vision*.
- [11] Ian Goodfellow, Jean Pouget-Abadie, Mehdi Mirza, Bing Xu, David Warde-Farley, Sherjil Ozair, Aaron Courville, and Yoshua Bengio. 2014. Generative Adversarial Nets. In *Neural Information Processing Systems*.
- [12] Liang-Yan Gui, Yu-Xiong Wang, Xiaodan Liang, and José MF Moura. 2018. Adversarial geometry-aware human motion prediction. In *European Conference on Computer Vision*.
- [13] Sepp Hochreiter and Jürgen Schmidhuber. 1997. Long short-term memory. *Neural computation* 9, 8 (1997), 1735–1780.
- [14] Catalin Ionescu, Dragoș Papava, Vlad Olaru, and Cristian Sminchisescu. 2014. Human3.6M: Large Scale Datasets and Predictive Methods for 3D Human Sensing in Natural Environments. *Transactions on Pattern Analysis and Machine Intelligence* 36, 7 (2014), 1325–1339.
- [15] Nal Kalchbrenner, Lasse Espeholt, Karen Simonyan, Aaron van den Oord, Alex Graves, and Koray Kavukcuoglu. 2016. Neural machine translation in linear time. *arXiv preprint arXiv:1610.10099* (2016).
- [16] Diederik P Kingma and Max Welling. 2014. Auto-encoding variational bayes. In *International Conference on Learning Representations*.

Long-Term Video Generation of Multiple Futures Using Human Poses

- [17] Alex X Lee, Richard Zhang, Frederik Ebert, Pieter Abbeel, Chelsea Finn, and Sergey Levine. 2018. Stochastic Adversarial Video Prediction. *arXiv preprint arXiv:1804.01523* (2018).
- [18] Michael Mathieu, Camille Couprie, and Yann LeCun. 2016. Deep multi-scale video prediction beyond mean square error. In *International Conference on Learning Representations*.
- [19] Mehdi Mirza and Simon Osindero. 2014. Conditional generative adversarial nets. *arXiv preprint arXiv:1411.1784* (2014).
- [20] Alejandro Newell, Kaiyu Yang, and Jia Deng. 2016. Stacked hourglass networks for human pose estimation. In *European Conference on Computer Vision*.
- [21] Katsunori Ohnishi, Shohei Yamamoto, Yoshitaka Ushiku, and Tatsuya Harada. 2018. Hierarchical Video Generation From Orthogonal Information: Optical Flow and Texture. In *Proceedings of the Thirty-Second AAAI Conference on Artificial Intelligence*.
- [22] Alec Radford, Luke Metz, and Soumith Chintala. 2016. Unsupervised representation learning with deep convolutional generative adversarial networks. In *International Conference on Learning Representations*.
- [23] Olaf Ronneberger, Philipp Fischer, and Thomas Brox. 2015. U-Net: Convolutional Networks for Biomedical Image Segmentation. In *Medical Image Computing and Computer-Assisted Intervention*.
- [24] Florian Schroff, Dmitry Kalenichenko, and James Philbin. 2015. Facenet: A unified embedding for face recognition and clustering. In *Computer Vision and Pattern Recognition*.
- [25] Graham W. Taylor, Geoffrey E Hinton, and Sam T. Roweis. 2007. Modeling Human Motion Using Binary Latent Variables. In *Neural Information Processing Systems*.
- [26] Ashish Vaswani, Noam Shazeer, Niki Parmar, Jakob Uszkoreit, Llion Jones, Aidan N. Gomez, Lukasz Kaiser, and Illia Polosukhin. 2015. Attention is all you need. In *Neural Information Processing Systems*.
- [27] Ruben Villegas, Jimei Yang, Yuliang Zou, Sungryull Sohn, Xunyu Lin, and Honglak Lee. 2017. Learning to Generate Long-term Future via Hierarchical Prediction. In *International Conference on Machine Learning*.
- [28] Carl Vondrick, Hamed Pirsiavash, and Antonio Torralba. 2016. Generating Videos with Scene Dynamics. In *Neural Information Processing Systems*.
- [29] Jacob Walker, Kenneth Marino, Abhinav Gupta, and Martial Hebert. 2017. The pose knows: Video forecasting by generating pose futures. In *International Conference on Computer Vision*.
- [30] Jack M Wang, David J Fleet, and Aaron Hertzmann. 2008. Gaussian process dynamical models for human motion. *Transactions on Pattern Analysis and Machine Intelligence* 30, 2 (2008), 283–298.
- [31] Yichao Yan, Jingwei Xu, Bingbing Ni, Wendong Zhang, and Xiaokang Yang. 2017. Skeleton-aided articulated motion generation. In *ACM International Conference on Multimedia*.